Experimental Study of the Rate of OH + HO_2 → H_2O + O_2 at High Temperatures Using the Reverse Reaction

Zekai Hong,* Subith S. Vasu, David F. Davidson, and Ronald K. Hanson

Department of Mechanical Engineering Stanford University, Stanford, California 94305, USA

Received: January 25, 2010; Revised Manuscript Received: March 17, 2010

The rate constant of the reaction OH + HO_2 → H_2O + O_2 (1) can be inferred at high temperatures from measurements of the rate of its reverse reaction H_2O + O_2 → OH + HO_2 (−1). In this work, we used laser absorption of both H_2O and OH to study the reverse reaction in shock-heated H_2O/O_2/Ar mixtures over the temperature range 1600−2200 K. Initial H_2O concentrations were determined using tunable diode laser absorption near 2.5 μm, and OH concentration time-histories were measured using UV ring dye laser absorption near 306.7 nm. Detailed kinetic analysis of the OH time-history profiles yielded a value for the rate constant k_1 of $(3.3 \pm 0.9) \times 10^{13}$ [cm^3 mol^{-1} s^{-1}] between 1600 and 2200 K. The results of this study agree well with those reported by Srinivasan et al. (Srinivasan, N.K.; Su, M.-C.; Sutherland, J.W.; Michael, J.V.; Ruscic, B. *J. Phys. Chem. A* **2006**, *110*, 6602−6607) in the temperature regime between 1200 and 1700 K. The combination of the two studies suggests only a weak temperature dependence of k_1 above 1200 K. Data from the current study and that of Keyser (Keyser, L.F. *J. Phys. Chem.* **1988**, *92*, 1193−1200) at lower temperatures can be described by the k_1 expression proposed by Baulch et al. (Baulch, D.L.; Cobos, C.J.; Cox, R.A.; Esser, C.; Frank, P.; Just, Th.; Kerr, J.A.; Pilling, M.J.; Troe, J.; Walker, R.W.; Warnatz, J. *J. Phys. Chem. Ref. Data* **1992**, *21*, 411), $k_1 = 2.89 \times 10^{13} \exp(252/T)$ [cm^3 mol^{-1} s^{-1}]. However, it should be noted that some previous studies suggest a k_1 minimum around 1250 K (Hippler, H.; Neunaber, H.; Troe, J. *J. Chem. Phys.* **1995**, *103*, 3510−3516) or 1000 K (Kappel, C.; Luther, K.; Troe, J. *Phys. Chem. Chem. Phys.* **2002**, *4*, 4392−4398).

1. Introduction

The reaction OH + HO_2 → H_2O + O_2 (1) plays an important role in combustion chemistry. It is a major HO_2 termination path in lean combustion,[1,2] and it is responsible for the depletion of both OH and HO_2 radicals in burnt gases.[3] The reaction has a very strong influence on the lift-off height of turbulent methane−air flames even at atmospheric pressure.[4] In addition, recent studies have shown that hydrocarbon ignition times at high pressures show a very strong negative sensitivity to this reaction.[5,6] The reaction also plays an important role in atmospheric chemistry as it is regarded as a dominant chain termination for OH and HO_2 radicals, both of which catalyze ozone destruction in the upper atmosphere.[7−12] Despite its importance, only a handful of experimental studies of this reaction have been conducted at elevated temperatures.[3,13−17]

An Arrhenius plot of previous measurements of k_1 conducted at high temperatures is shown in Figure 1. In the early work by Goodings and Hayhurst,[3] k_1 values were estimated from temperature measurements of burner flames. More quantitative measurements of k_1 were later carried out using laser absorption of OH or HO_2. Hippler et al.[16] reported a k_1 minimum near 1250 K in a study of the H_2O_2 decomposition system. A more recent measurement by Kappel et al.,[17] again in the H_2O_2 decomposition system, found the rate minimum to be near 1000 K. Thus, it is possible that a rapid increase in k_1 over the small temperature range from 970 to 1220 K may be responsible for the large spread of data seen by Kappel et al.[17] shown in Figure 1. In these two studies, OH and HO_2 radicals were intermediate species of H_2O_2 decomposition. However, no such strong temperature dependence of k_1 was observed by Srinivasan et al.[13] in a reaction system containing NO_2 and C_2H_5I. Heated by reflected shock waves, C_2H_5I rapidly decomposes into C_2H_5 and I radicals, with C_2H_5 subsequently decomposing to form H and C_2H_4. These H radicals initiate reactions by attacking NO_2 to yield OH; the generated OH radicals in turn react with NO_2 to form HO_2. With the coexistence of OH and HO_2 in the system, Srinivasan et al.[13] were able to study the reaction OH + HO_2 → H_2O + O_2. An average value for $k_1 = (4.0 \pm 1.6) \times 10^{13}$ [cm^3 mol^{-1} s^{-1}] was reported between 1200 and 1700 K.

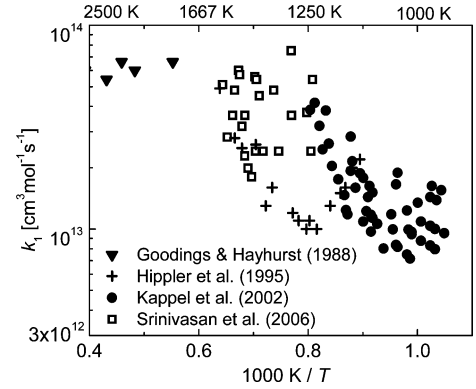

Figure 1. Arrhenius plot of the rate constant of the reaction OH + HO_2 → H_2O + O_2. Large scatter is seen in the measured reaction rate values.

Almost all the previous studies of the reaction OH + HO_2 → H_2O + O_2 involved OH and HO_2 as the reactants. To the authors' knowledge, this reaction has not been studied in its reverse direction using H_2O and O_2 as reactants, although the

* To whom correspondence should be addressed.

10.1021/jp100739t
Published on Web 04/14/2010

reaction scheme should be much simpler and more direct. Computer simulations using a detailed chemical kinetics mechanism, GRI-Mech 3.0,[18] indicate that the formation of OH radicals in instantaneously heated H_2O/O_2 mixtures is predominantly controlled by the kinetics of the reaction. Here, we apply this reverse-reaction strategy in a shock tube using UV laser absorption of OH.

2. Experimental Setup

The experimental setup of the current study is very similar to the one used in a previous study[19] and is only briefly reviewed here.

Experiments were carried out in a high-purity shock tube with inner diameter of 14.13 cm. The driven section of the shock tube is 8.54 m long, and the driver section is 3.35 m long. Test mixtures were instantaneously heated by reflected shock waves, with conditions determined using standard normal-shock relations. Uncertainty in the temperature immediately following shock reflection, T_5, was $\pm 0.8\%$.[19−21]

Compared to the small uncertainties in initial reflected shock temperature and pressure, T_5 and P_5, temperature and pressure variations at longer test times can be larger. These pressure and temperature variations are normally caused by facility-related nonideal effects in shock tubes, such as boundary layer growth and shock attenuation. In the current study, these facility-related effects have been suppressed by adding inserts to the shock-tube driver section.[22] With this modification, overall postshock pressure fluctuation for all tests was kept below $\pm 2\%$, and the corresponding long-time overall temperature variation was less than $\pm 0.8\%$. This same driver insert technique has been successfully applied to reduce temperature uncertainty in several previous chemical kinetics studies in our laboratory.[19,20,23]

Test mixtures were prepared by passing a stream of premixed 1% O_2/Ar (Praxair) through a flask filled with degassed pure water. The flask was kept in an ice−water bath to maintain a low water vapor pressure. The flow rate of the carrier gas (premixed O_2/Ar) was adjusted to achieve a water concentration near 1.5% in the test mixtures, thereby avoiding condensation in the shock tube. The test mixture was directed into the driven section of the shock tube from a filling port near the endwall. Total filling pressures in the driven section (P_1) were between 0.04 and 0.12 atm.

Actual H_2O mole fractions in the test mixtures were determined using laser absorption of a H_2O transition at 2550.96 nm (3920.09 cm^{-1}). A collimated laser beam from a distributed feedback (DFB) diode laser (Nanoplus GmbH) was transmitted through the shock tube at 2 cm from the endwall. The laser wavelength was fixed at the center of the H_2O absorption feature. Details of the development and use of this H_2O diagnostic can be found in Hong et al.[19,20]

OH concentration time-histories were measured using CW laser absorption of the $R_1(5)$ line of the OH $A^2\Sigma^+ - X^2\Pi$ (0,0) band near 306.7 nm. The absorption coefficient of the OH radical is well established and known to within $\pm 5\%$.[21,24,25] Fundamental 613.4 nm light was generated using a Coherent Verdi laser pumping a Spectra-Physics 380 ring-dye laser operating with Rhodamine R6G dye. This radiation was frequency-doubled to yield UV light (1−2 mW) using a temperature-tuned AD*A crystal. The 306.7 nm laser was then transmitted through the shock tube at the same location as the H_2O diagnostic, 2 cm from the endwall. Further details of the OH ring-dye laser absorption diagnostic are available from other studies in our laboratory.[19,21]

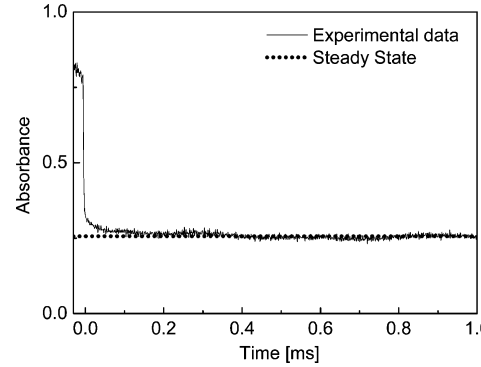

Figure 2. Using the time-history of the laser absorbance near 2.5 μm, the steady-state H_2O concentration was determined to be 1.3%. The composition of the test mixture can be calculated to be 1.3% H_2O/0.99% O_2/97.71% Ar. Initial reflected shock conditions: 1880 K, 1.74 atm.

3. Results and Discussion

3.1. Test Mixture Composition. Figure 2 shows the time-history of the H_2O laser absorbance obtained at 1880 K and 1.74 atm, which exhibits features common to all tests. Laser absorbance A is defined in the Beer−Lambert Law as $A = -\ln(I_v/I_v^o)$, where I_v^o and I_v are the incident and transmitted laser intensities, respectively. Detailed discussions on laser absorbance can be found in ref 20.

The apparent overshoot in H_2O laser absorption that occurs within a few microseconds near time zero is a result of the vibrational relaxation of H_2O. The equilibrium temperature upstream of the reflected shock wave is 984 K in this example case. After the passage of the reflected shock wave, the H_2O vibrational mode eventually reaches equilibrium with the translational and rotational modes, and a temperature equilibrium is reestablished at 1880 K. Because the fraction of H_2O molecules in the lower energy state of the absorption transition peaks around 400 K,[20,26] the H_2O absorbance decreases dramatically from 984 to 1880 K. A vibrational relaxation study of H_2O in argon bath gas by Kung and Center[27] suggests that the characteristic time of the process is approximately 0.5 μs, consistent with the rapid fall in absorbance near time zero that defines the passage of the reflected shock.

Following the initial sharp decline in laser absorption, the temperature continues to decline over the next 100 μs to a final steady-state value because of the slower vibrational relaxation time scale for O_2 in this mixture.

Little fluctuation in H_2O concentration is seen after 0.1 ms. The estimated overall uncertainty in the H_2O concentration is $\pm 10\%$, which also includes the uncertainty in the absorption cross-section. The steady-state H_2O concentration, which is the mean value between 0.1 and 1 ms, was used to calculate test mixture composition. By putting emphasis on the OH temporal profile after 0.1 ms, error in k_1 due to this simplification can be minimized.

Although the temperatures of core flow behind reflected shock waves were between 1600 and 2200 K in the current study, the walls of the shock tube were still at room temperature. Condensation on room temperature walls was avoided by using mixtures with water vapor partial pressure (behind reflected shock) less than the saturation pressure of water vapor at room temperature (0.032 atm).

3.2. Determination of the Rate of the Reaction $OH + HO_2 \rightarrow H_2O + O_2$ (k_1). Using a kinetics model, the OH sensitivity coefficient can be calculated with the Senkin kinetics suite.[28] The sensitivity coefficient is defined as the partial derivative of

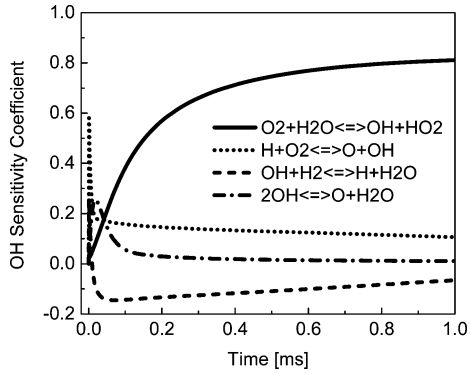

Figure 3. OH sensitivity plot at conditions of Figure 2.

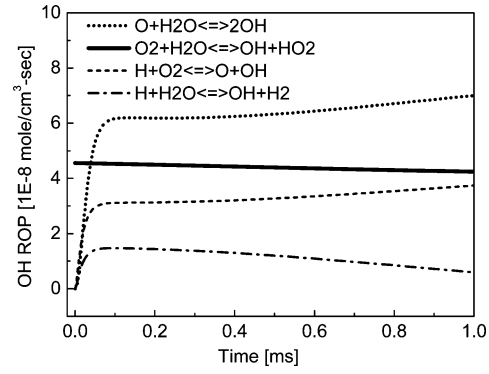

Figure 4. Rate of production analysis (ROP) of OH at conditions of Figure 2.

a species mole fraction with respect to the rate constant parameter A of a reaction, normalized by the maximum species mole fraction and the rate constant parameter A

$$\alpha_{ij}(t) = (\mathrm{d}X_j/X_j^{\max})/(\mathrm{d}A_i/A_i)$$

where X_j is the mole fraction of species j and A_i is the temperature-independent factor of the rate constant of reaction i.

Figure 3 is the corresponding OH sensitivity plot for the conditions of Figure 2. The sensitivity coefficient was calculated using an updated version of GRI-Mech 3.0.[18] The parameters updated in the mechanism are: (1) the OH heat of formation,[21,29] (2) the HO_2 heat of formation,[30] and (3) the rate constant for the reaction $H + O_2 \rightarrow O + OH$.[23] In addition, the rate expression for the reaction $OH + HO_2 \rightarrow H_2O + O_2$ was replaced by its reverse counterpart.

OH formation shows the largest sensitivity to the rate of the reverse reaction $H_2O + O_2 \rightarrow OH + HO_2$ (k_{-1}). Therefore, k_{-1} can be accurately evaluated by changing this rate in the chemical kinetics model to best fit experimental OH time-histories. k_{-1} can then be readily converted to k_1 through the equilibrium constant: $K_c = k_1/k_{-1}$. Once a k_{-1} value was experimentally determined, the sensitivity coefficient was recalculated with the updated k_{-1}. The sensitivity plot in Figure 3 was calculated using the experimentally determined k_{-1}.

It is also evident from the sensitivity analysis that only a few reactions control the kinetics of a simple reaction system such as the one under investigation. Among these controlling reactions, the dominant one ($O_2 + H_2O \rightarrow OH + HO_2$) is the target of this study. The rate expressions for the reaction $OH + H_2 \rightarrow H + H_2O$ are essentially identical for all commonly used mechanisms,[18,31−33] and are based on the study by Michael et al.[34] However, for the reaction $2OH \rightarrow H_2O + O$, the Li et al.[31] and the Ó Conaire et al.[32] mechanisms use the rate expression from an early study,[35] whereas GRI-Mech 3.0[18] uses the one recommended by a more recent study.[36] In addition, GRI-Mech 3.0 was updated with the rate constant for the reaction $H + O_2 \rightarrow O + OH$ from a very recent study.[23] The updated GRI-Mech 3.0 thus reflects recent improvements in the H_2/O_2 mechanism and was selected as the base mechanism to analyze experiment data in the present study. It should also be pointed out that the selection of the base mechanism only has very minor effects on the determination of k_1, as OH formation is predominantly controlled by the kinetics of the target reaction.

The rate of production analysis (ROP) was carried out as well for the conditions of Figure 2, as presented in Figure 4. Although there are three other major channels to produce OH besides the target reaction in its reverse direction $H_2O + O_2 \rightarrow OH + HO_2$, this reaction is the initiation and rate-limiting step for OH formation. Near time zero, OH is produced almost exclusively via $H_2O + O_2 \rightarrow OH + HO_2$. Shortly after the initial radical pool is established, OH production through other reaction channels rapidly accelerates, with each ROP contribution achieving plateau levels within ~100 μs. That is a clear indication that $H_2O + O_2 \rightarrow OH + HO_2$ is the rate-limiting step, and it explains that OH shows dominant sensitivity to this reaction.

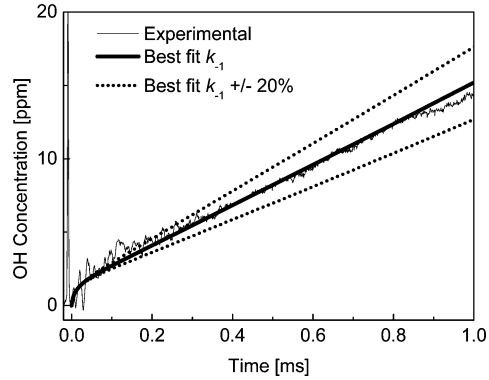

Figure 5. Comparison of experimental and Senkin calculated OH profiles using best-fit k_{-1} with the effect of ±20% variation on k_{-1} at conditions of Figure 2.

Using the Beer−Lambert law, laser attenuation at 306.7 nm due to the absorption of OH radicals can be converted to OH temporal profiles. Shown in Figure 5 is the OH time-history obtained from the same experiment as the H_2O laser absorbance in Figure 2. The experimental data are compared with the best-fit profile calculated using a k_{-1} value of 3.1×10^6 [cm^3 mol^{-1} s^{-1}]. Two OH profiles calculated using 120 and 80% of the best-fit k_{-1} are presented on the same plot. The fitting uncertainty of k_{-1} is conservatively estimated to be ±10%.

A near-linear increase in OH concentration was observed over 1 ms without showing an apparent sign of fall off to gradually reach a plateau, suggesting that the equilibrium OH level might be much higher than the experimental observation at 1 ms. A thermodynamic calculation using the latest heats of formation for OH[21,29] and HO_2[30] indicates that the equilibrium OH concentration is 173 ppm for this example. In addition, a kinetics calculation using GRI-Mech 3.0[18] predicts that it takes approximately 50 ms to achieve the equilibrium OH level.

However, a small nonlinear rise was observed between 0 and 0.1 ms. This behavior can be attributed to residual impurities in the shock tube, despite efforts to keep the shock tube very clean and evacuated between shock wave experiments to

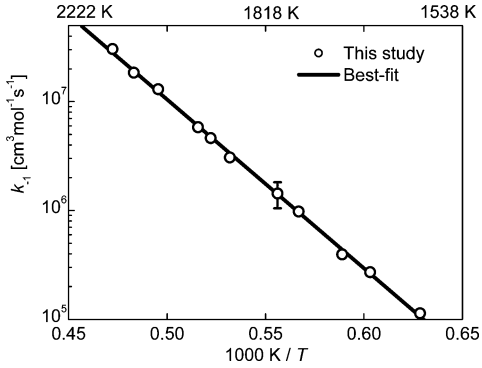

Figure 6. Arrhenius plot of experimentally determined k_{-1} between 1600 and 2200 K. The best-fit to the measured k_{-1} values (solid line) can be expressed as $k_{-1} = 6.0 \times 10^{14}\exp(-35\,720/T)$ [cm^3 mol^{-1} s^{-1}].

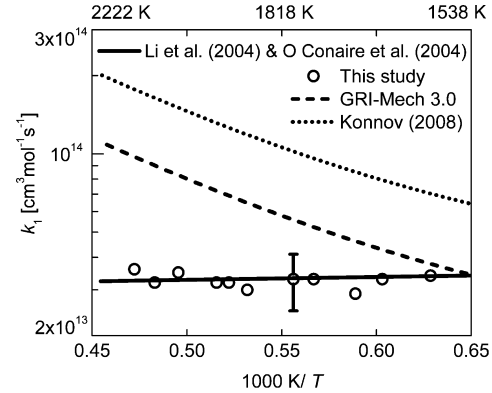

Figure 7. Arrhenius plot of experimentally determined k_1 between 1600 and 2200 K. The k_1 expressions used in recent reaction mechanisms are also shown. Dash: GRI-Mech 3.0;[18] dot: Konnov mechanism;[33] solid: Li et al. mechanism[31] and Ó Conaire et al. mechanism.[32]

pressures ~10^{-7} Torr. An experiment was conducted at similar conditions but excluding H_2O from the test mixture. We still observed a very similar small rapid rise in OH concentration at early times, confirming that the target reaction is not responsible for this brief nonlinear OH rise.

The residual impurity issue has been encountered repeatedly in previous studies.[21,23] At temperatures of interest in this study, trace amounts of hydrocarbon impurities are converted into OH radicals almost instantly by vastly abundant O_2. In practice, the impurity effects are modeled by artificially including H atoms in the initial mixture used for the numerical simulation. For the example case shown, 0.7 ppm of H atom was included in calculating the OH profiles in Figure 5 and the OH sensitivity coefficients in Figure 3.

3.3. Uncertainty Analysis. It is seen from Figure 3 that OH formation shows some sensitivity to three reactions other than the target of this study. (1) The uncertainty associated with the reaction rate of H + O_2 → O + OH is less than ±5%[23] over the entire temperature range of the interest of this work. The resulting uncertainty in k_{-1} is less than ±2%, and can be neglected here. (2) OH formation shows sensitivity only to the reaction 2OH → O + H_2O between 0 and 0.1 ms. As was discussed in the previous section, we rely heavily on the OH time-history after 0.1 ms for the assessment of k_{-1}. Yet again, the error introduced by uncertainty in the rate of the reaction 2OH → O + H_2O can be eliminated by not including the experimental data obtained between 0 and 0.1 ms. (3) The reaction OH + H_2 → H_2O + H has negative sensitivity to OH formation over the entire test time and needs to be carefully evaluated for uncertainty in its reaction rate. The review by Baulch et al.[37] assigns a factor of 2 uncertainty to the reaction rate of OH + H_2 → H_2O + H. Our analysis reveals that k_{-1} is subject to only about ±4% uncertainty because of this interference reaction.

As briefly mentioned in Section 2, uncertainties in H_2O and OH absorption cross sections were estimated to be ±10 and ±5%, respectively, resulting in a k_{-1} uncertainty of ±12%. In addition, the temperature uncertainty has been assessed to be ±23 K in this temperature range, which introduces approximately ±22% uncertainty in inferred k_{-1} values. Combining uncertainties from all error sources—such as the best-fitting procedure (±10%), absorption cross sections of OH and HO_2 (±12%), interfering reactions (±4%), and temperature (±22%)—the overall uncertainty for k_{-1} is ±27%.

3.4. Arrhenius Plot. Experiments were conducted over a wide temperature range from 1600 to 2200 K. Figure 6 summarizes all experimental k_{-1} values. The best-fit to all the data points yields an expression for k_{-1}: $6.0 \times 10^{14}\exp(-35720/T)$ [cm^3 mol^{-1} s^{-1}]. The equilibrium constant of the reaction can be calculated using the current thermochemical data,[18,21,29,30] yielding $K_c = 0.0642\exp(35\,420/T)$ between 1600 and 2200 K. The entropy change for the reaction OH + HO_2 → O_2 + H_2O is small, and therefore, the exponential part of the equilibrium constant is predominantly the difference in formation enthalpies. Note that the activation energy for the reverse reaction O_2 + H_2O → OH + HO_2 is almost identical to the difference in formation enthalpies. This suggests that there is no or only a small energy barrier on the reaction path of the forward reaction.

The measured k_{-1} values are converted into k_1 using the equilibrium constant, and are plotted in Figure 7. No apparent temperature dependence of k_1 was found between 1600 and 2200 K. The solid line in the figure represents the average of $k_1 = (3.3 \pm 0.9) \times 10^{13}$ [cm^3 mol^{-1} s^{-1}] from this study, in good agreement with $k_1 = (4.0 \pm 1.6) \times 10^{13}$ [cm^3 mol^{-1} s^{-1}] between 1237 and 1554 K as reported by Srinivasan et al.[13]

For comparison, the expressions for k_1 used in commonly employed mechanisms[18,31−33] are also plotted in Figure 7. The rate constant expression adopted in the models by Li et al.[31] and Ó Conaire et al.[32] is based on the early reviews by Baulch et al.[38,39] On the other hand, GRI-Mech 3.0 and the Konnov model[33] estimate the rate constant of the reaction OH + HO_2 → H_2O + O_2 based on low-temperature studies[7−10] and the high-temperature study by Hippler et al.[16] The two latter kinetic mechanisms assign relatively large positive activation energies (>17 kcal/mol) to k_1 at high temperatures. As temperature rises, the agreement between this study and the Konnov model/GRI-Mech 3.0 degrades.

Figure 8 presents both high- and low-temperature experimental data. Previous studies[7−12] at low temperatures agree on the general trend and suggest a slight negative activation energy. From Figure 8, it is evident that the k_1 expression given by the early Baulch et al. reviews,[38,39] $k_1 = 2.89 \times 10^{13}\exp(252/T)$ [cm^3 mol^{-1} s^{-1}] (which is identical to the rate coefficient used by Li et al.[31] and Ó Conaire et al.[32]), matches well with the results of the current study and some obtained at low temperatures.[7,8,10,11] However, discrepancy exists between the high-temperature data for $T > 1000$ K. The studies by Hippler et al.[16] and Kappel et al.[17] suggest a strong temperature dependence of k_1. Activation energies as high as 17.5 kcal/mol have been used in kinetic compilations[18,33,37] to account for the strong k_1 temperature dependency between 1300 and 2000 K.

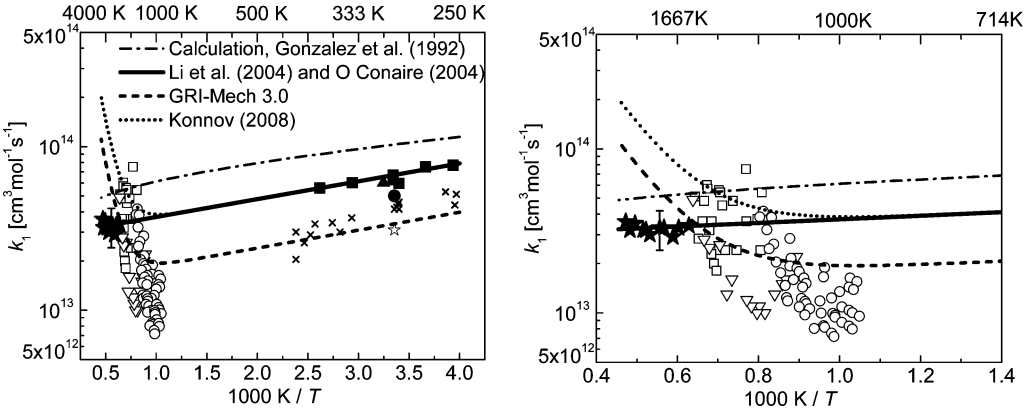

Figure 8. Arrhenius plots for k_1. Results from this study are compared to previous experimental data (★- this study; □- Srinivasan et al.;[13] ▽- Hippler et al.;[16] ○- Kappel et al.;[17] ■- Keyser;[8] ▲- Cox et al.;[11] and Lii et al.;[10] ●- Schwab et al.;[7] ☆- Rozenshtein et al.;[12] ×- Sridharan et al.[9] k_1 expressions adopted in some commonly used reaction mechanisms[18,31−33]are also presented. The ab initio calculation by Gonzalez et al.[41] can be scaled by 0.61 to well match the rate constant expression used in Li et al.[31] and Ó Conaire et al.[32] kinetic mechanisms.

This study does not support this strong temperature dependency, at least for temperatures above 1600 K.

It should be noted that although the k_1 expression used by Li et al.[31] and Ó Conaire et al.[32] well represents the results of the current study, the study by Srinivasan et al.,[13] and those at low temperatures,[7,8,10,11] caution should be exercised when extending the expression beyond the experimentally confirmed regions, particularly, between 400 and 1200 K. This is because a deep and narrow rate constant minimum may exist close to 1250[16] or 1000 K[17] as a result of "the formation of intermediate complexes".[16]

Calculating the ab initio surfaces are difficult for the reaction of $OH + HO_2 \rightarrow H_2O + O_2$.[40−44] It is therefore difficult to theoretically justify the anomalous temperature dependency as observed by Hippler et al.[16] and Kappel et al.[17] A calculation that uses collision theory to estimate a rough upper bound for the reaction $OH + HO_2$ on the triplet energy surface has been carried out.[13] The calculation assumes that the reaction is barrier-free and leads to a conclusion that the rate constant k_1 is expected to level off at high temperatures, even if the narrow minimum may exist near 1000 K. Therefore, the lack of strong temperature dependence at high temperatures as found in the current study does not completely rule out the possibility of a minimum k_1 near 1000 K. Independent study in the temperature range of 900−1200 K is needed to confirm this unusually deep and narrow rate constant minimum.

Gonzalez et al. carried out the most thorough ab initio calculations on the reaction between OH and HO_2, both on the singlet[40] and triplet[41] potential energy surfaces. They concluded that the reaction on the singlet energy surface, $OH + HO_2 \leftrightarrow HOOOH \rightarrow H_2O + O_2$, is unimportant for pressures up to a few atmospheres and for temperatures below 2500 K.[40]

The reaction proceeds predominantly on the triplet energy surface, $OH + HO_2 \leftrightarrow HO\cdots HO_2 \rightarrow H_2O + O_2$, as an H-abstraction reaction. Gonzalez et al.[41] found that the hydrogen-bond in the complex $HO\cdots HO_2$ is too weak to produce a significant pressure dependence. Their ab initio calculations reveal that the rate of the target reaction is not controlled by the transition state on the triplet energy surface. Therefore, the reaction rate is essentially the rate of formation of the hydrogen-bonded complex, which is referred to as the capture rate and is controlled by the long-range interaction between OH and HO_2. The capture rate was calculated using vibrationally/rotationally adiabatic theory and found to be $k_1 = 7.05 \times 10^{13} (T/300)^{-0.21} \exp(113/T)$ [cm^3 mol^{-1} s^{-1}],[41] as illustrated by the dash-dot curve in Figure 8. The negative temperature dependence is mainly explained by the fact that the electronic partition function of one of the reactants, OH radical, increases at elevated temperatures due to a low-lying energy state $^2\Pi_{1/2}$, which is only 0.41 kcal/mol[45] above the ground state $^2\Pi_{3/2}$.

Although the vibrationally/rotationally adiabatic theory calculations by Gonzalez et al.[41] capture the negative temperature dependence of k_1 accurately, the predicted values are consistently higher than experimental data. Gonzalez et al.[41] scaled down their calculation results to match the low temperature experimental data by Keyser[8] to yield a new expression $k_1 = 4.28 \times 10^{13} (T/300)^{-0.21} \exp(113/T)$ [cm^3 mol^{-1} s^{-1}]. The rescaling leads to k_1 values (not shown in Figure 8) very close to those calculated using the expression recommended by early Baulch reviews[38,39] between 200 and 2000 K.

4. Conclusions

Small amounts of H_2O vapor were blended with premixed 1% O_2/Ar bath gas to form H_2O/O_2/Ar mixtures. Using tunable diode laser absorption of H_2O near 2.5 μm, the test mixture compositions were evaluated directly. These mixtures were shock-heated to temperatures between 1600 and 2200 K to study OH time-histories using laser absorption at 306.7 nm.

OH formation is predominantly controlled by the reverse reaction $H_2O + O_2 \rightarrow OH + HO_2$ (k_{-1}). Because k_1 is directly proportional to k_{-1} through the equilibrium constant: $K_c = k_1/k_{-1}$, the values of k_1 were determined by varying them in a modified version of GRI-Mech 3.0 to generate OH profiles that best-fit the experimental observations. k_1 was found to be $(3.3 \pm 0.9) \times 10^{13}$ [cm^3 mol^{-1} s^{-1}] between 1600 and 2200 K. Srinivasan et al.[13] reported an average k_1 value of $(4.0 \pm 1.6) \times 10^{13}$ [cm^3 mol^{-1} s^{-1}] between 1237 and 1554 K, in good agreement with the current study. The combination of the two studies suggests only a weak temperature dependence of k_1 above 1200 K.

The k_1 expression recommended by Baulch et al.,[38,39] $k_1 = 2.89 \times 10^{13} \exp(252/T)$ [cm^3 mol^{-1} s^{-1}], accurately represents the measurements of the current study, the study by Srinivasan et al.,[13] and those at low temperatures,[7,8,10,11] However, as noted above, there is still some uncertainty about the behavior of this reaction rate constant in the temperature range of 400−1200 K. An independent study of k_1 in the temperature range of 900−1200 K would help to resolve this uncertainty.

Acknowledgment. This work was supported by the National Science Foundation under award No. 0649936, the Department

of Energy, Office of Basic Energy Sciences, with Dr. Wade Sisk as technical monitor, and the Department of Energy [National Nuclear Security Administration] under Award No. NA28614.

References and Notes

(1) Peeters, J.; Mahnew, G. *Symposium (International) on Combustion* **1973**, *14*, 133–146.
(2) Petersen, E. L.; Davidson, D. F.; Hanson, R. K. *Combust. Flame* **1999**, *117*, 272–290.
(3) Goodings, J. M.; Hayhurst, A. N. *J. Chem. Soc. Faraday Trans. 2* **1988**, *84*, 745–762.
(4) Gkagkas, K.; Lindstedt, R. P. *Proc. Combust. Inst.* **2007**, *31*, 1559–1566.
(5) Vasu, S. S.; Davidson, D. F.; Hanson, R. K. *Combust. Flame* **2009**, *156*, 736–749.
(6) Petersen, E. L.; Röhrig, M.; Davidson, D. F.; Hanson, R. K.; Bowman, C. T. *Proc. Combust. Inst.* **1996**, *26*, 799–806.
(7) Schwab, J. J.; Brune, W. H.; Anderson, J. G. *J. Phys. Chem.* **1989**, *93*, 1030–1035.
(8) Keyser, L. F. *J. Phys. Chem.* **1988**, *92*, 1193–1200.
(9) Sridharan, U. C.; Qiu, L. X.; Kaufman, F. *J. Phys. Chem.* **1984**, *88*, 1281–1282.
(10) Lii, R.-R.; Gorse, R. A., Jr.; Sauer, M. C., Jr.; Gordon, S. *J. Phys. Chem.* **1980**, *84*, 819–821.
(11) Cox, R. A.; Burrows, J. P.; Wallington, T. J. *Chem. Phys. Lett.* **1981**, *84*, 217–221.
(12) Rozenshtein, V. B.; Gershenzon, Yu. M.; Il'in, S. D.; Kishkovitch, O. P. *Chem. Phys. Lett.* **1984**, *112*, 473–478.
(13) Srinivasan, N. K.; Su, M.-C.; Sutherland, J. W.; Michael, J. V.; Ruscic, B. *J. Phys. Chem. A* **2006**, *110*, 6602–6607.
(14) Hippler, H.; Troe, J.; Willner, J. *J. Chem. Phys.* **1990**, *93*, 1755–1760.
(15) Hippler, H.; Troe, J. *Chem. Phys. Lett.* **1992**, *192*, 333–337.
(16) Hippler, H.; Neunaber, H.; Troe, J. *J. Chem. Phys.* **1995**, *103*, 3510–3516.
(17) Kappel, Ch.; Luther, K.; Troe, J. *Phys. Chem. Chem. Phys.* **2002**, *4*, 4392–4398.
(18) Smith, G. P.; Golden, D. M.; Frenklach, M.; Moriarty, N. W.; Eiteneer, B.; Goldenberg, M.; Bowman, C. T.; Hanson, R. K.; Song, S.; Gardiner, W. C.; Lissianski, V. V.; Qin, Z. GRI-Mech 3.0; http://www.me.berkeley.edu/grimech/ (accessed November 12, 2009).
(19) Hong, Z.; Cook, R. D.; Davidson, D. F.; Hanson, R. K. *J. Phys. Chem. A* **2010**, doi: 10.1021/jp100204z.
(20) Hong, Z.; Farooq, A.; Barbour, E. A.; Davidson, D. F.; Hanson, R. K. *J. Phys. Chem. A* **2009**, *113*, 12919–12925.
(21) Herbon, J. T.; Hanson, R. K.; Golden, D. M.; Bowman, C. T. *Proc. Combust. Institute* **2002**, *29*, 1201–1208.
(22) Hong, Z.; Pang, G. A.; Vasu, S. S.; Davidson, D. F.; Hanson, R. K. *Shock Waves* **2009**, *19*, 113–123.
(23) Hong, Z.; Davidson, D. F.; Barbour, E. A.; Hanson, R. K. *Proc. Combust. Institute* **2010**, accepted.
(24) Vasudevan, V.; Davidson, D. F.; Hanson, R. K. *J. Phys. Chem. A* **2005**, *109*, 3352–3359.
(25) Davidson, D. F.; Oehlschlaeger, M. A.; Herbon, J. T.; Hanson, R. K. *Proc. Combust. Institute* **2002**, *29*, 1295–1301.
(26) Ethan, A. B. *Modeling and Laser-Based Sensing of Pulsed Detonation Engines. Ph.D. Dissertation*; Stanford University: Stanford, CA, 2009. http://thermosciences.stanford.edu/pdf/TSD-177.pdf (accessed November 15, 2009).
(27) Kung, R. T. V.; Center, R. E. *J. Chem. Phys.* **1975**, *62*, 2187–2194.
(28) Lutz, A. E.; Kee, R. J.; Miller, J. A. *Senkin: A FORTRAN Program for Predicting Homogeneous Gas Phase Chemical Kinetics with Sensitivity Analysis; Report No. SAND87−8248*; Sandia National Laboratory: Albuquerque, NM, 1988.
(29) Ruscic, B.; Wagner, A. F.; Harding, L. B.; Asher, R. L.; Feller, D.; Dixon, D. A.; Peterson, Y.; Song, K. A.; Qian, X. M.; Ng, C. Y.; Liu, J. B.; Chen, W. W. *J. Phys. Chem. A* **2002**, *106*, 2727–2747.
(30) Ruscic, B.; Pinzon, R. E.; Morton, M. E.; Srinivasan, N. K.; Su, M.-C.; Sutherland, J. W.; Michael, J. V. *J. Phys. Chem. A* **2006**, *110*, 6592–6601.
(31) Li, J.; Zhao, Z.; Kazakov, A.; Dryer, F. L. *Int. J. Chem. Kinet.* **2004**, *36*, 566–575.
(32) O Conaire, M.; Curran, H. J.; Simmie, J. M.; Pitz, W. J.; Westbrook, C. K. *Int. J. Chem. Kinet.* **2004**, *36*, 603–622.
(33) Konnov, A. A. *Combust. Flame* **2008**, *152*, 507–528.
(34) Michael, J. V.; Sutherland, J. W. *J. Phys. Chem.* **1988**, *92*, 3853–3857.
(35) Sutherland, J. W.; Patterson, P. M.; Klemm, R. B. *Symposium (International) on Combustion* **1991**, *23*, 51–57.
(36) Wooldridge, M. S.; Hanson, R. K.; Bowman, C. T. *Int. J. Chem. Kin.* **1994**, *26*, 389–401.
(37) Baulch, D. L.; Bowman, C. T.; Cobos, C. J.; Cox, R. A.; Just, Th.; Kerr, J. A.; Pilling, M. J.; Stocker, D.; Troe, J.; Tsang, W.; Walker, R. W.; Warnatz, J. *J. Phys. Chem. Ref. Data* **2005**, *34*, 757–1397.
(38) Baulch, D. L.; Cobos, C. J.; Cox, R. A.; Esser, C.; Frank, P.; Just, Th.; Kerr, J. A.; Pilling, M. J.; Troe, J.; Walker, R. W.; Warnatz, J. *J. Phys. Chem. Ref. Data* **1992**, *21*, 411.
(39) Baulch, D. L.; Cobos, C. J.; Cox, R. A.; Frank, P.; Hayman, G.; Just, Th.; Kerr, J. A.; Murrells, T.; Pilling, M. J.; Troe, J.; Walker, R. W.; Warnatz, J. *J. Phys. Chem. Ref. Data* **1994**, *23*, 847–1033.
(40) Gonzalez, C.; Theisen, J.; Zhu, L.; Schlegel, B.; Hase, W. L.; Kaiser, E. W. *J. Phys. Chem.* **1991**, *95*, 6784–6792.
(41) Gonzalez, C.; Theisen, J.; Zhu, L.; Schlegel, B.; Hase, W. L.; Kaiser, E. W. *J. Phys. Chem.* **1992**, *96*, 1767–1774.
(42) Jackels, C. F.; Phillips, D. H. *J. Chem. Phys.* **1986**, *84*, 5013–5024.
(43) Toohey, D. W.; Anderson, J. G. *J. Phys. Chem.* **1989**, *93*, 1049–1058.
(44) Cremer, D. *J. Chem. Phys.* **1978**, *69*, 4456–4471.
(45) Clary, D. C.; Werner, H. J. *Chem. Phys. Lett.* **1984**, *112*, 346–350.

JP100739T